Proceedings of the ASME 2009 28th International Conference on Ocean, Offshore and Arctic Engineering
OMAE2009
May 31 - June 5, 2009, Honolulu, Hawaii, USA

OMAE2009-79579

'INVERSE' CONCEPT: WAVE ENERGY GENERATION BY MOTION AND GREEN WATER MAXIMISATION

Bas Buchner and Frederick Jaouen

MARIN (Maritime Research Institute Netherlands)
Haagsteeg 2 / P.O. Box 28
6700 AA Wageningen, The Netherlands
b.buchner@MARIN.NL, f.jaouen@MARIN.NL

ABSTRACT

This paper presents the initial investigations into the 'Inverse' concept for wave energy conversion, based on the maximisation of motions and green water. The 'Inverse' concept combines aspects of 'overtopping', 'heaving' and 'pitching' wave energy conversion concepts, but also adds specific aspects such as the use of green water. Instead of reducing the motions and green water as is done in normal offshore hydrodynamics, the 'Inverse' concepts tries to maximise the motions and green water to generate energy from the waves. Results are presented of frequency domain calculations for the motion (de-) optimisation. Improved Volume Of Fluid (iVOF) simulations are used to simulate the green water flow on the deck. It is concluded that the potential of the 'Inverse' concept is clear. As a result of the double connotation of the word 'green', this renewable energy concept could also be called the 'green water' concept. Further work needs to be carried out on the further optimisation of the concept.

BACKGROUND

Although there has been interaction between the fields of wave energy conversion and offshore engineering, in the view of the authors more co-operation can be fruitful. This paper is our first contribution in this direction. It makes use of the experience and tools developed for offshore hydrodynamics in the development of a new wave energy conversion concept. This concept is called 'Inverse', as it inverses the objectives of offshore engineering. Instead of reducing the motions and green water of monohull offshore structures (such as FPSOs), the 'Inverse' concept maximises the motions and green water as a means of extracting energy from the waves (see Figure 1). However, as part of this process, the learnings and methods from normal offshore hydrodynamics and naval architecture are very useful.

The 'Inverse' concept as presently presented is by no means a final concept. It is developed as a vehicle for open discussion and exchange of ideas in this interesting field. It is also our humble contribution from an offshore engineering perspective to the field of renewable energy, realising that we are beginners in this field and have not studied the vast amount of papers in the wave energy converter field completely and in detail. Still we believe that a contribution from the field of offshore hydrodynamics and offshore engineering can be useful for an improved design, engineering, installation and operation of wave energy converters.

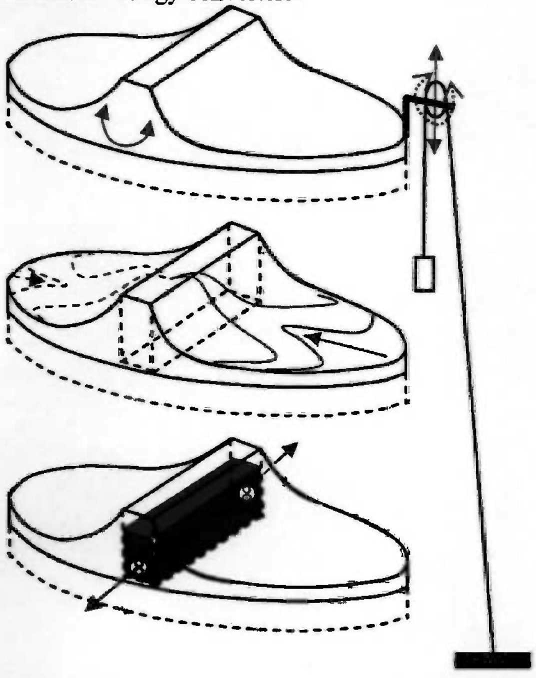

Figure 1: Operation of the 'Inverse' wave energy converter concept in three stages (or processes)

INTRODUCTION OF THE 'INVERSE' CONCEPT

Basically, the 'Inverse' concept is a weathervaning small freeboard vessel with a water reservoir in centre, as shown in the schematic Figure 1. Figure 1 shows the different stages in the concept to clarify its operation (in reality these stages are parallel interacting processes). From top to bottom:

1. Maximum vertical motions at the bow by maximising the pitch motions. Due to the large arm with respect to the centre of rotation (~'midships'), the vertical motions at the point of the electrical generator at the bow are not just the heave motion (as in the case of a buoy), but also this contribution of the pitch motion. The tethered weathervaning mooring keeps the structure head into the main wave environment.
2. Green water on the deck (with low freeboard) fills the water reservoir in centre. During research into the effect of green water on ship-type offshore structures [1], it was found that the flow onto the deck from the front and the sides of the bow, concentrates in a high velocity jet over the centreline of the vessel. This process can be seen in Figures 2 and 3. The resulting velocity over the centreline of the deck can be 15 to 25 m/s. This green water is able to impose high loads on structures on the deck (see the last photograph in Figure 3), but is also able to climb the slope into the reservoir of the 'Inverse'concept. This process will alternately occur both at the bow and stern, although the effect on the bow will be slightly stronger.
3. The greenwater flows out of the reservoir through low water head turbines.

So the wave energy conversion is both a result of the motions at the bow and the green water flow out of the reservoir.

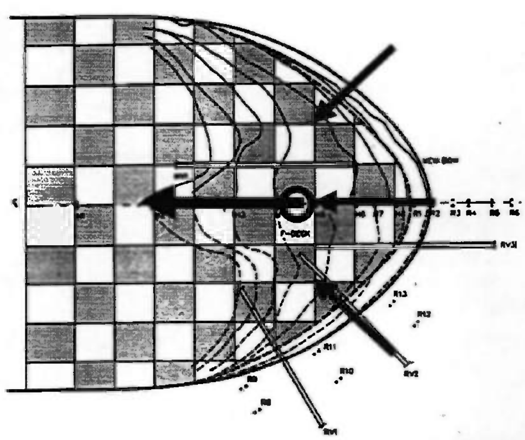

Figure 2: Green water flow onto the deck from the front and sides of the bow concentrates in a high velocity jet over the centreline of the vessel [1]

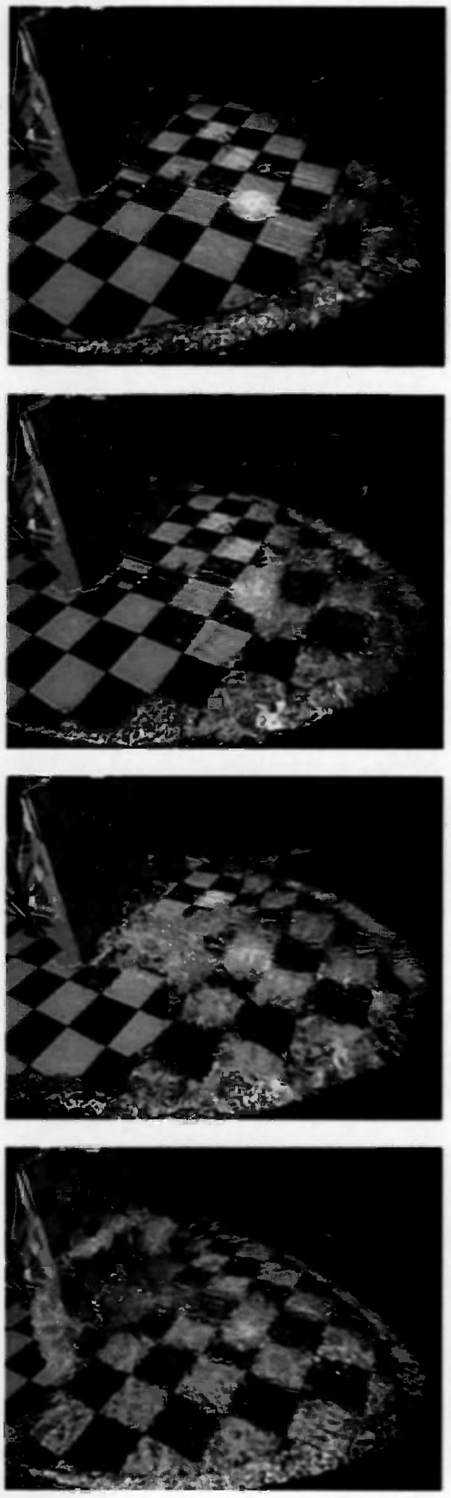

Figure 3: Green water on the deck of an FPSO [1]

'INVERSE' CONCEPT IN PERSPECTIVE

Let us now consider the 'Inverse' concept in the perspective of the available power in the waves and other wave energy conversion concepts.

The main challenge of all wave energy systems is to extract as much as possible energy from the waves. For this purpose it is important to know how much energy is actually present in the waves themselves. In long-crested deep water waves the wave energy flux per unit wave crest width is P (kW/m):

$$P = \frac{\rho g^2}{64\pi} H_s^2 T$$

H_s is the significant wave height (m), T the wave period (s), ρ the density of seawater (kg/m^3) and g gravity (m/s^2). So the power of the waves is proportional to the wave period and proportional to the square of the significant wave height. As an example: a 10 second wave period with a significant wave height of 3 metres results in a 45 kW wave power potential per metre crest width.

It will be clear that, due to its high density, water is capable of transferring a lot of energy compared to wind energy systems. Consequently even small wave energy devices are capable of producing energy. By nature wave energy concepts are also low-profile compared to wind energy systems, which minimises the visual distraction if placed off-shore.

The earliest serious attempts to generate energy from the waves date from the 1970's in the time of the oil crisis. The most famous system was the 'Salter's Duck' (or officially called 'Edinburgh Duck'). However, this system was never tested offshore. New wave energy devices include the 'Pelamis', the 'Archimedes Wave Swing' and the 'Wave Dragon', of which (prototype) systems actually operate.

In an excellent summary, [2] classifies the large amount of different concepts in different groups as follows:

- *Oscillating Water Column* concepts, which are open at the bottom. The vertical motion of the water inside the structure due to the waves alternatively pressurizes and depressurizes the air inside the structure generating a reciprocating flow through a turbine at the top. Typical examples are the 'Mighty Whale' (floating) and the 'Limpet' unit on Islay (fixed).
- *Overtopping* concepts, floating or fixed to the shore. They collect the water of incident waves in an elevated reservoir to drive one or more low head turbines. An example on an overtopping device is for instance the 'Wave Dragon'. With a wave reflector it focusses the wave towards a ramp to fill a higher-level reservoir. Also the shore-based 'Tapchan' system is an example of an overtopping concept.
- *Heaving* concepts, which can be both floating or submerged. The heave motion is converted by mechanical and/or hydraulic systems in linear or rotational motion for driving electrical generators. An example is the 'PowerBuoy'.
- *Pitching* concepts consist of a number of floating bodies, hinged together. The relative motions between the floating bodies are used to pump high-pressure oil through hydraulic motors, which drive electrical generators. The 'Pelamis' is a typical example of this concept.
- *Surging* concepts make use of the horizontal particle velocity in a wave. This drives a deflector or generates a pumping effect of a flexible bag facing the wave front. The 'WaveRoller' is a concept in this category.

All wave energy generation or conversion concepts are facing significant challenges:

- Waves are irregular in nature. Any seastate consists of a significant range of frequencies and directions and beside that the seastates themselves change strongly in time.
- It is difficult to develop a system with optimum efficiency for a wide range of wave heights and periods.
- The concept should be able to withstand survival conditions without damage.
- The transformation of an irregular wave frequency motion (around 0.1 Hz) of the waves through electrical generators to a frequenyc typically 500 times higher is a complex process.
- The energy has to be transferred to shore, typically through subsea cables.
- Like all (renewable and normal) offshore concepts, offshore installation, maintenance and removal can be complex and costly.

We will now consider the 'Inverse'concept in the light of the above perspective.

The 'Inverse'concept has elements of overtopping, heaving and pitching concepts:

- Compared to existing 'overtopping' concepts, the overtopping is not the result of wave focussing or run up, but caused by the dynamics of the green water on a moving deck.
- 'Heaving' concepts are typically smaller buoys, where the vertical motion is only a result of the heave motion of the buoy. The 'Inverse' concept makes use of the combined heave and pitch motion to generate maximum vertical motions at the location of the electrical generator.
- Compared to the 'pitching' concepts, the 'Inverse' concept does not make use of hinges and related submerged hydraulics to generate energy.
- No use was made so far of oscillating water column ideas, although this could be done by making use of the maximum vertical motions at the bow and stern as indicated in Figure 4.

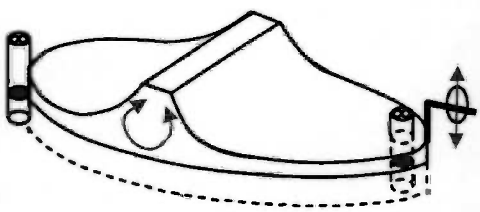

Figure 4: Potential use of oscillating water columns inside (as shown at the bow) or outside (as shown at the stern) in the 'Inverse' concept

Further the following strong points of the 'Inverse' concept can be mentioned:

- The structure is simple to build (by local shipyards).
- Easy transportation due to its ship-shaped hull. The concept is (almost) self installing after it has been towed to location. The sheaves of the electrical generator at the bow can be used to install the bottom anchor (foundation plate, suction anchor or drag anchor).
- The concept is removable for inshore maintenance and final removal (like FPSOs), which are larger challenges for fixed offshore windmills.
- Compared to smaller buoy systems, the required infrastructure will be limited (no complex grid of subsea lines required) for the same amount of energy.
- The system is weathervaning, keeping the bow head into the main wave environment
- The system can be used in deep and shallow water and is independent of the tides
- The length of the 'Inverse'concept will be chosen so that the period of maximum pitch excitation is close to the dominant wave period at the field location in moderate seastates. By ballasting it is possible to tune the pitch resonance period to combine the maximum wave excitation, natural period and wave period.
- In extreme weather conditions the wave periods will be longer and the short 'Inverse' concept will follow the wave slope. Further the highest waves will overtop the low freeboard structure. Though this results in extreme green water on the watertight structure, this reduces the motions, drift forces and mooring loads and protects the structure again excessive survival loads.

Based on the evaluation above, it was considered worthwile to investigate the concept further hydrodynamically. This will be done in the following phases:

1. Motion analysis and (de-)optimisation using frequency domain diffraction analysis
2. Maximisation of the green water on the deck using an improved Volume of Fluid (iVOF) method [3-5]
3. Time domain motion and mooring analysis, including the evaluation of the wave energy conversion potential

The present paper focusses on Phase 1 and the initial results of Phase 2. The full Phase 2 and Phase 3 will be performed in the next stage and will be reported in later papers.

'INVERSE' CONCEPT MOTION (DE-)OPTIMISATION

Methodology

The motion calculations were performed with MARIN's linear diffraction code DIFFRAC. DIFFRAC solves the linearised velocity potential problem using a three-dimensional source distribution technique. The mean wetted part of the vessel hull is approximated by a large number of panel elements. The distribution of source singularities on these panels forms the velocity potential describing the fluid flow around the vessel hull. The pressure distribution on the hull is calculated from the velocity potential. The added mass and damping coefficients, as well as the wave forces are then determined from the pressure distribution. All these calculations in DIFFRAC are carried out in the frequency domain. The added mass (a) and damping coefficients (b) and the wave load coefficients (exciting forces and moments) can be used to calculate the motion RAOs for the 6 components of the motions. As an example, the (uncoupled) equation of motion for pitch can be written as:

$$(I_{yy} + a_\theta)\ddot{\theta} + b_\theta\dot{\theta} + c_\theta\theta = M_\theta$$

As mentioned before, the length of the 'Inverse' concept will be chosen so that the period of maximum pitch excitation is close to the dominant wave periods at the field location in moderate seastates. As a starting point the length of the 'Inverse' concept was chosen at 60m. For normal ship-type offshore structures such as FPSOs, the pitch resonance period is typically much shorter than the period of maximum wave excitation, resulting in limited pitch motions. However, for the 'Inverse' concept the mass moment of inertia can be chosen such that the natural pitch period shifts to the period of maximum wave excitation, resulting in more resonant-type motion. At resonance the inertia and spring terms in the equation of motion are cancelling eachother, resulting in a response dominated by wave excitation and system damping (which includes energy generation).

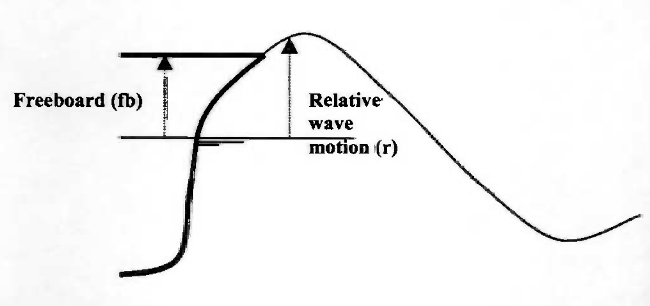

Figure 5: Definition of relative wave motion (r) and freeboard with respect to the waterline in calm water (fb)

Variations

To maximise the pitch motions (local vertical motions at position of the electrical generator at the bow) and relative wave motions (Figure 5, as input to the green water), a range of structural shapes and dimensions was investiaged.

The first group (Figure 6) consisted of 3 different ellipsoids with different length over beam (L/B) ratios of 3, 5 and 7:

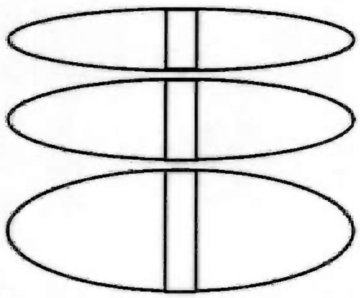

Figure 6: Ellipsoids with different L/B ratios of 3, 5 and 7

The second group (Figure 7) included more triangular structures, as it was concluded in [1] that triangular structures can have (un)favourable large motion characteristics and that the triangular shape of the deck can result in a really focussed green water flow on the deck.

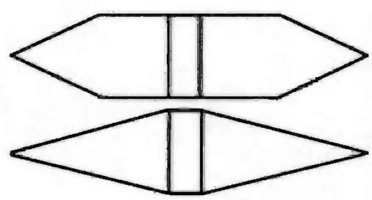

Figure 7: More triangular hull shapes

All structures had simple vertical sides over the full depth of the structure. In Figures 8, 9 and 10 an overview is given of the element distributions used for the diffraction analysis.

Another variation often investigated in naval architecture is the ratio between the beam and draft (B/T) of the structure. With increasing draft the wave damping decreases, whereas the wave excitating is not varying that much. This typically results in higher heave and pitch motions with larger drafts of ship-type structure (with extremely large drafts, as used for Spars, the wave excitation reduces significantly, almost eliminating the heave motions). For all the ellipsoids, three B/T-ratios are used of 3 (highest draft), 5 and 7 (smallest draft). In a later stage one ellipsoid was added with a B/T ratio of 1 (Body 0). For one triangular structure also a B/T variation was applied.

For the radius of pitch gyration (kyy) a value of 15m (25% of L) was chosen as base case. For Body 1 (Ellipsoid, L/B=3, B/T=3) and Body 12 (Triangular, L/B=3, B/T=3) a realistic variation of radii of gyration was applied (using ballast) of kyy=10, 12, 15, 18 and 20. Table 1 gives an overview of the resulting main dimensions of all variations with its reference colours and symbols that will be in the presentation of the results.

			B/T	L/B	L	B	T	D	Displ	GMl	GMt
			[-]	[-]	[m]	[m]	[m]	[m]	[tonnes]	[m]	[m]
Body 0	●	Ellipsoid	1.0	3.0	60.0	20.0	20.0	21.0	19321.0	11.2	1.2
Body 1	▪	Ellipsoid	3.0	3.0	60.0	20.0	6.7	7.7	6440.3	33.6	3.7
Body 2	◊	Ellipsoid	5.0	3.0	60.0	20.0	4.0	5.0	3864.2	56.1	6.2
Body 3	Δ	Ellipsoid	7.0	3.0	60.0	20.0	2.9	3.9	2760.1	78.5	8.7
Body 4	x	Ellipsoid	3.0	5.0	60.0	12.0	4.0	5.0	2318.5	56.0	2.2
Body 5		Ellipsoid	5.0	5.0	60.0	12.0	2.4	3.4	1391.1	93.4	3.7
Body 6		Ellipsoid	7.0	5.0	60.0	12.0	1.7	2.7	993.6	130.7	5.2
Body 7	+	Ellipsoid	3.0	7.0	60.0	8.6	2.9	3.9	1182.9	78.5	1.6
Body 8		Ellipsoid	5.0	7.0	60.0	8.6	1.7	2.7	709.7	130.8	2.6
Body 9		Ellipsoid	7.0	7.0	60.0	8.6	1.2	2.2	507.0	183.1	3.7
Body 10	□	Triangle	3.0	5.0	60.0	12.0	4.0	5.0	2214.0	46.8	2.5
Body 11	-	Triangle	3.0	5.0	60.0	12.0	4.0	5.0	1574.4	37.6	1.7
Body 12	*	Triangle	3.0	3.0	60.0	20.0	6.7	7.7	4375.5	22.6	2.8

Table 1: Main particulars of all variations

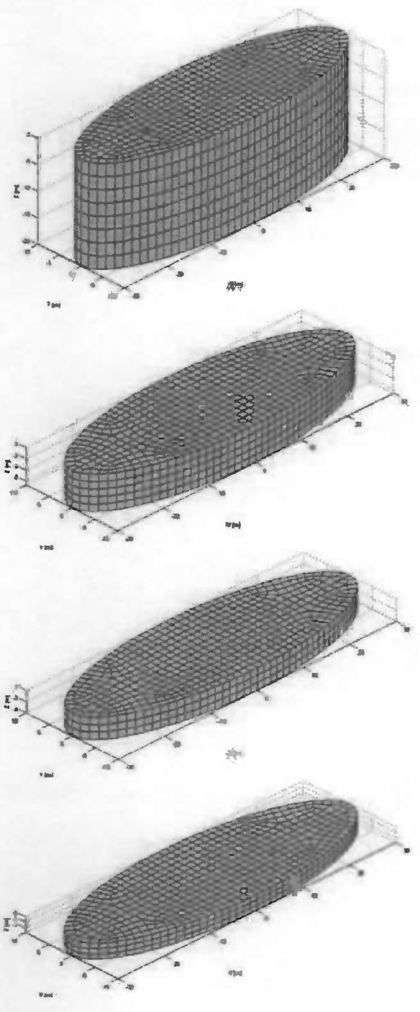

Figure 8: Element distributions with an L/B of 3 and B/T of 1, 3, 5 and 7 (from top to bottom: Body 0, 1, 2 and 3)

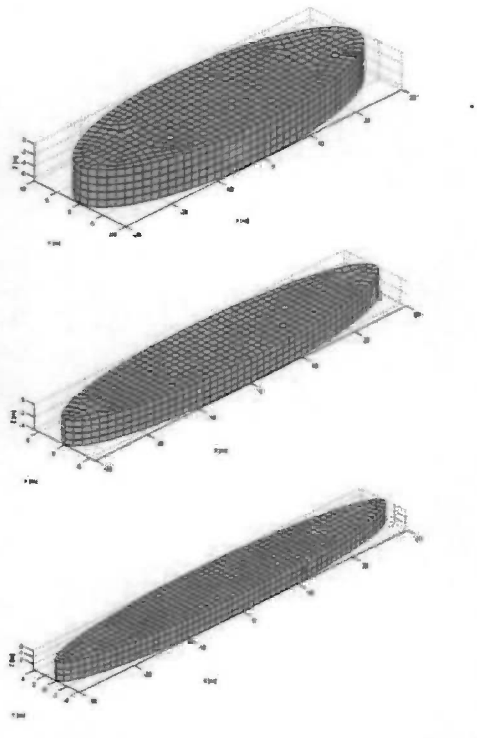

Figure 9: Element distributions with an L/B of 3, 5 and 7 and B/T of 3 (from top to bottom: Body 1, 4 and 7)

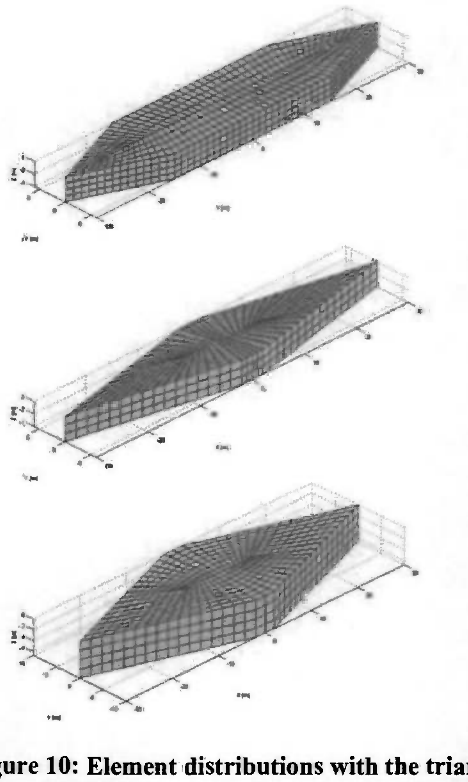

Figure 10: Element distributions with the triangular structures (from top to bottom: Body 10, 11 and 12)

Results

In the next few pages an overview will be given of the results of the systematic series of calculations carried out. By consistent colour codes and symbols it is tried to keep the overview as good as possible. The results of some bodies (5, 6, 8 and 9) are not presented to limit the size of the paper and because the results of the other bodies cover the trends found for these bodies.

As a starting point, Figure 11 presents the pitch motion RAOs for different groups of bodies. The upper graph presents the results of the B/T variation for bodies 1, 2 and 3 with the same width. It will be clear that the body with the largest draft (body 1) shows the largest pitch response (peak at almost 9 degrees per metre wave amplitude). This is a result of the lowest pitch (wave) damping combined with an almost similar wave exciting moment as for the other drafts. This will be discussed later in more detail. The middle graphs shows the sensitivity for the L/B ratio (with constant B/T ratio) for bodies 1, 4 and 7. It will be clear from this graph that the widest structure (body 1) has the largest pitch response. For triangular bodies 11 and 12 the pitch response (bottom graph) is even more extreme. For body 12 a peak response of 19 degrees/m is observed, clearly a result of resonant behaviour.

Figure 12 shows a similar comparison for the heave response. These graphs show that only body 1 and 12 really show resonant heave response around 0.8 rad/s.

Figure 14 combines the heave motions for bodies 1, 2, 3 and 12 with the pitch motions, to determine the absolute vertical motion at the generator point at the bow of the structure (assumed at +35m, 5 m in front of the bow). This Figure confirms the large motions of bodies 1 and 12. In a wave of 1.0m, the generator point of body 1 moves more than 5.0m and body 12 even more than 10.0m. This is without the effect of a generator extracting energy for the system and reducing the motions accordingly. Also non-linear effects (expected with these large motions) are neglected in this calculations.

Figure 13 then presents the relative wave motion RAOs at the bow of the structure. Some interesting trends can be observed:

- For bodies 1, 2 and 3 the same type of trend is observed as for the pitch motions. This can be well understood because of the strong relation between (out of phase) pitch motion and relative wave motion.
- In long waves the structures follow the wave slope (no relative wave motions), in short waves the structure is not moving anymore and the relative wave motion is purely a result of the incoming wave (RAO value of 1.0) and the reflected wave (RAO value of +1.0 for full bows and +0.0 for thin triangular bows). This trend is clear in the results. The high frequency limit for bodies 1, 2 and 3 (top graph) is close to 2.0 (almost standing waves), for the less wide bodies 4 and 7 this reduces (middle graph) and for the thin triangular bows 10, 11 and 12 it is close to one.

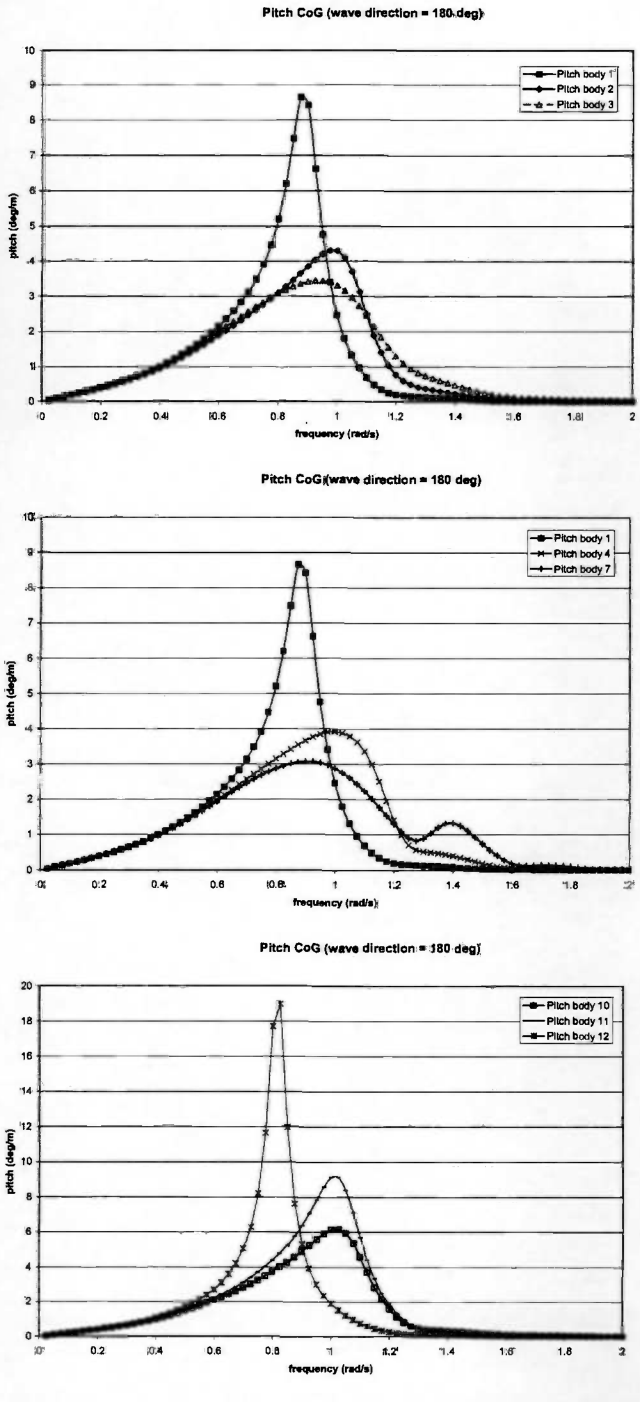

Figure 11: Pitch motion RAOs for different groups of bodies

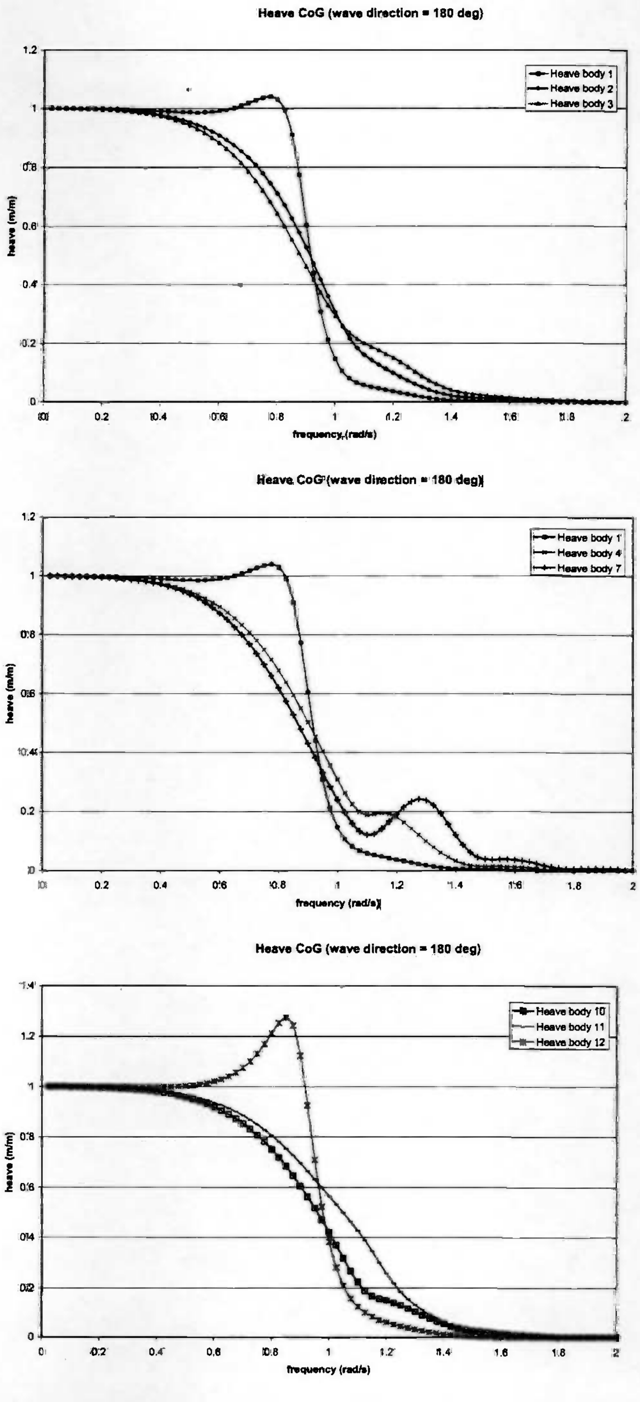

Figure 12: Heave motion RAOs for different groups of bodies

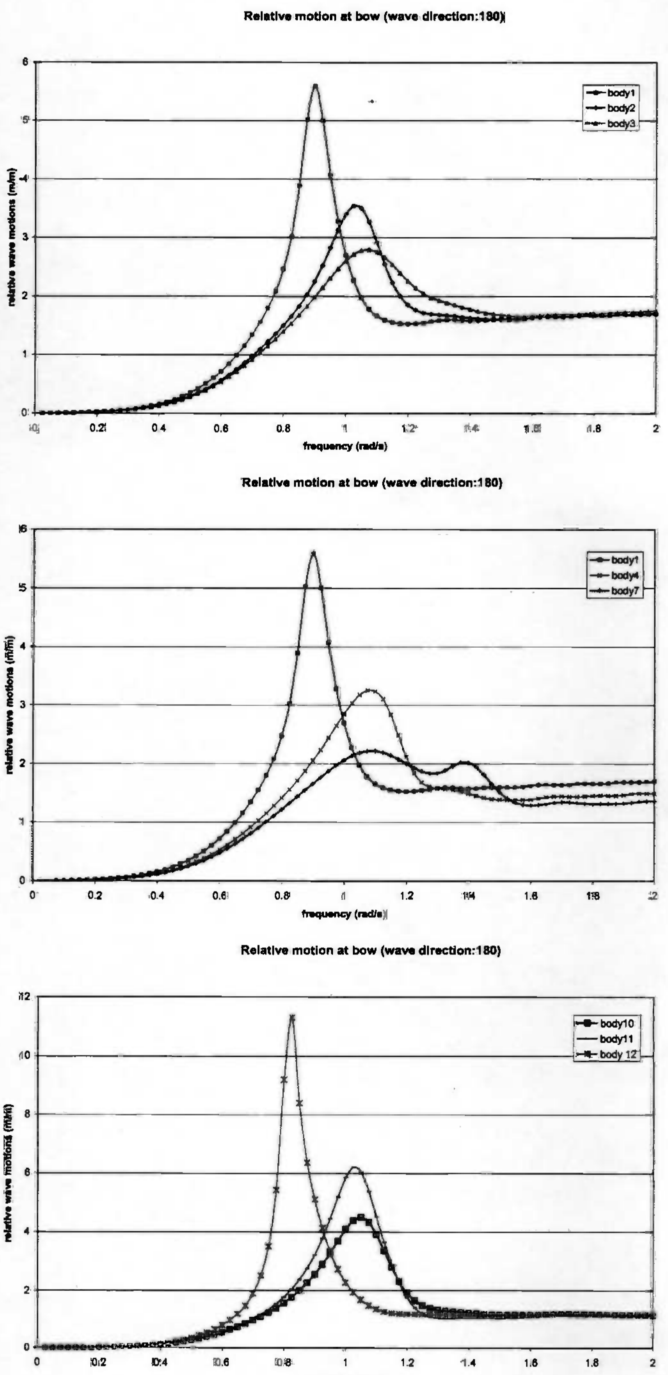

Figure 13: Relative wave motion RAOs for different groups of bodies

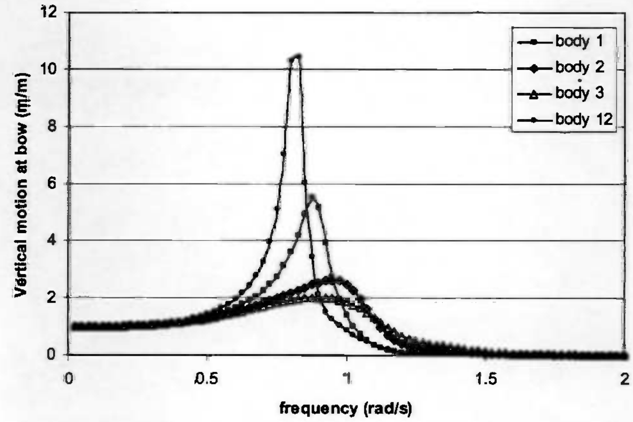

Figure 14: Vertical motion at the bow for bodies 1, 2, 3 and 12

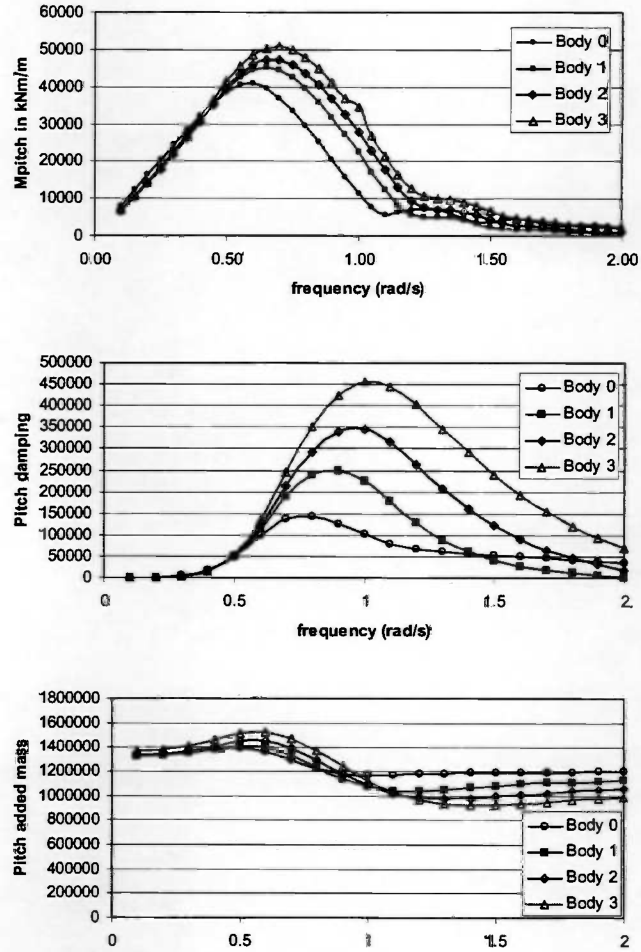

Figure 15: Wave exciting moment, pitch damping and pitch added mass for body 0, 1, 2 and 3

- The relative wave motions for bodies 1 and 12 are remarkable. With an input wave of 1.0m, the relative motion of body 1 is 5.5m and for body 12 this is even 11m. It should be noted that this neglects the possible effects of the green water on the motions [1].

It is important to note that the motion response of the structure as observed, is a resonant response to the wave excitation. At resonance, the spring and inertia terms in the equation of motion cancel each other, which implies that the response is determined by the balance between the wave excitation and damping only (it should be noted that in the present calculations the damping effects of energy generators is neglected, so that the actual motion response will be lower).

Therefore, it is now time to investigate the background of the observed differences in more detail. In this we will focus on elliptical bodies 1-3 and triangular body 12. Figure 15 shows the pitch exciting moment, pitch damping and pitch added mass (from top to bottom) for body 1 (B/T=3), 2 (B/T=5) and 3 (B/T=7.0). In a later stage a body 0 was added with an even large draft (B/T=1). The following typical trends can be observed:

- The pitch exciting moment (top graph) reduces only slightly with increasing draft. Only from B/T=3 (body 1) to B/T=1 (body 0) there is a signficant reduction in wave excitation. The reduction of the wave excitation is explained by the reduced orbital motions at the level of the bottom of the structure (exponential decay).
- The reduction of the wave damping (middle graph) is, however, much stronger with increasing drafts. This is a result of the fact that the wave damping (radiation damping) strongly reduces when the distance of the bottom of the structure to the free surface increases.
- For the structure with the largest draft, the high frequency limit of the damping becomes larger again. This is a result of the contribution of the vertical sides of the structure to the wave damping, which for a structure with a larger draft becomes significant.
- The added mass becomes more and more constant with increasing draft, as the free surface effects in the added mass become less important.

So the increased response at increasing draft can be explained by the fact that the wave excitation reduces less with the increasing draft than the wave damping. A reduced wave damping is attractive as this implicates that less energy is dissipated by wave radiation and can be used for actual wave energy conversion. For the moment body 1 is used for further work (as the draft of body 0 is considered to be a bit extreme, also considering the costs of steel).

Figures 16 and 17 now present the wave exciting pitch moment and pitch damping for bodies 1, 4 and 7 (above) and bodies 10, 11 and 12 (below). Compared to body 1, the less wide bodies 4 and 7 have a smaller wave exciting moment as expected. The wave damping also reduces, but at a lesser rate.

Considering the large motion response of body 12 in Figure 14, at first sight it is surprising that the wave exciting moment on this body is so low compared to (for instance) body 1. This lower excitation can be understood from the triangular shape of the bow. The larger response can be explained by the even smaller pitch damping as can be observed in Figure 17.

So it is concluded that the actual motion response is a result of the balance between the wave exciting moment and (wave) damping. However, this ratio is dependent on the frequency as well. Further, the actual motion response is determined by the resonant period, in which the spring (GM) and inertia terms play important roles. To understand these relations one step better, Figure 18 shows the pitch motions, pitch wave excitation (/10000) and pitch damping (/30000) for bodies 1, 2, 3 and 12 (from top to bottom). For sake of comparison, the same vertical scale has been used. The following can be observed if we study these graphs carefully:

- The pitch excitation peaks at a wave frequency of 0.7 rad/s (T=8.98s), which represents a deep water wave length of approximately 125m. This is surprisingly long considering the length of the structures of 60m. The length of the 'Inverse'concept can be adjusted to the range of existing wave periods at a certain location. The present 60m of length can be considered as an upper limit based on these results.
- The reducing response with decreasing draft of bodies 1, 2 and 3 is clear from the graphs. However, this is not just an effect of the increasing wave damping, but also an issue of natural periods. Table 2 shows the longitudinal and transverse GM values and natural pitch periods for these bodies (with kyy=15m for all). The natural periods can be determined from the following expressions:

$$T_{natural} = 2\pi\sqrt{\frac{I_{yy} + a_{\theta}}{\rho g \nabla GM}}$$

$$I_{yy} = k_{yy}^2 \rho \nabla$$

It will be clear from this table that the lighter bodies 2 and 3 have smaller natural periods. As a result, their maximum pitch response occurs further away from the point of maximum pitch exciting moment (and minimum pitch damping).

Body	GMl	GMt	Tnatural	ωnatural
	[m]	[m]	[s]	[rad/s]
1	33.65	3.72	6.84	0.92
2	56.08	6.21	6.03	1.04
3	78.51	8.69	5.69	1.10

Table 2: Longitudinal and transverse GM values and natural pitch periods and frequencies for bodies 1, 2 and 3.

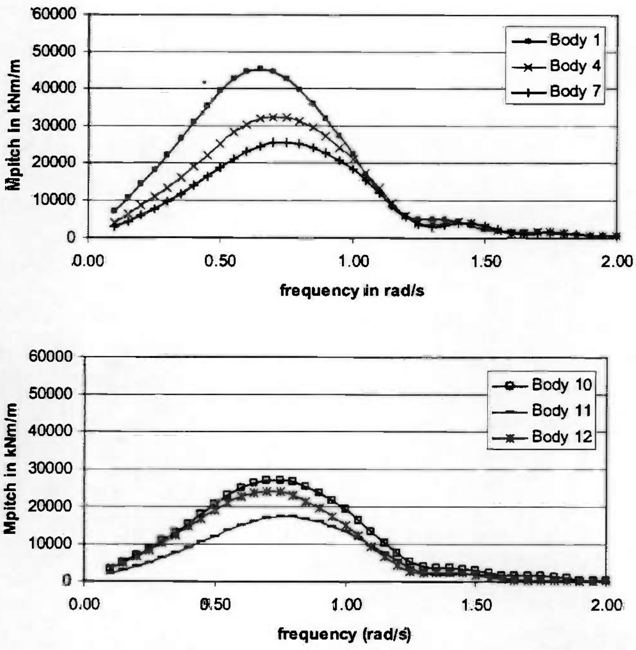

Figure 16: Wave exciting moment for bodies 1, 4 and 7 (above) and bodies 10, 11 and 12 (below)

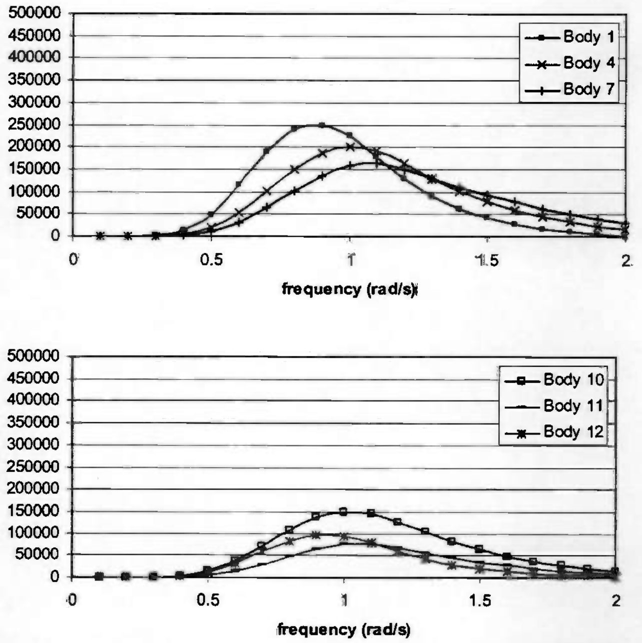

Figure 17: Pitch damping bodies 1, 4 and 7 (above) and bodies 10, 11 and 12 (below)

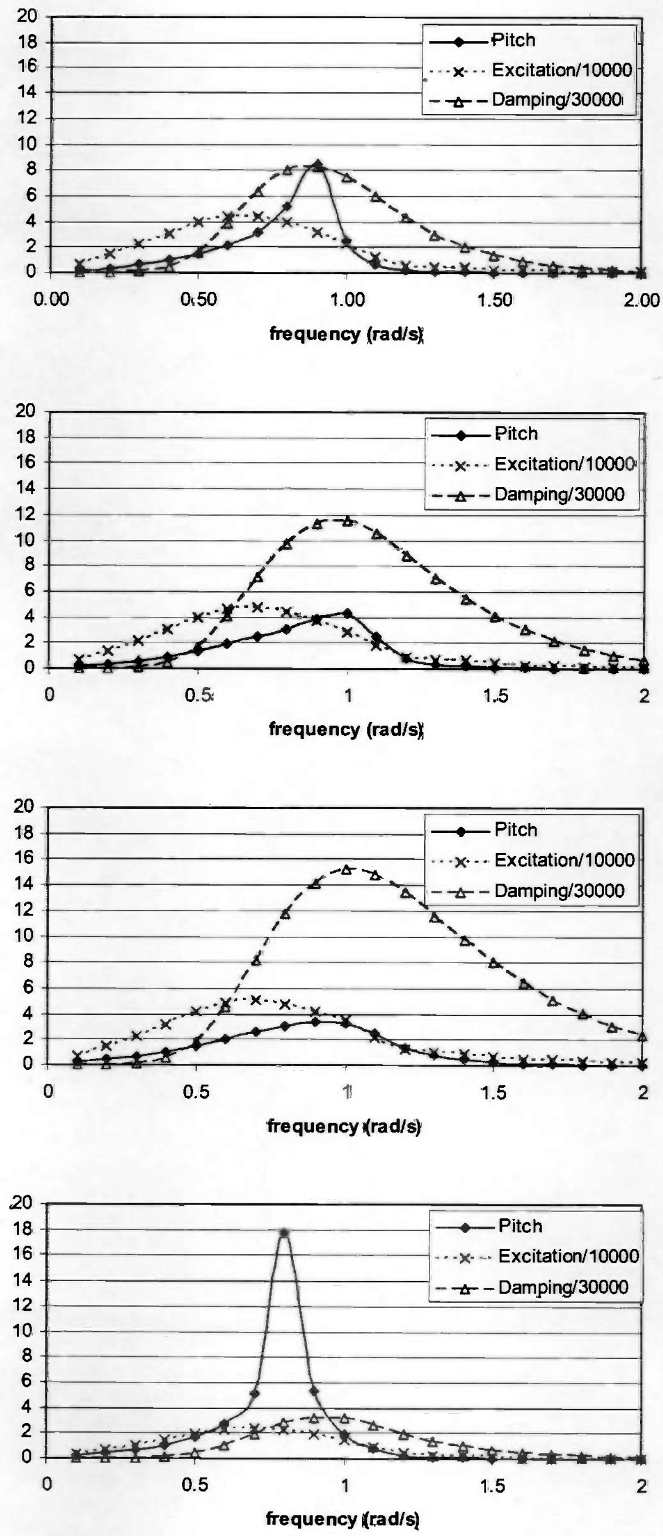

Figure 18 Pitch motions, pitch excitation (/10000) and pitch damping (/30000) for bodies 1, 2, 3 and 12 (from top to bottom)

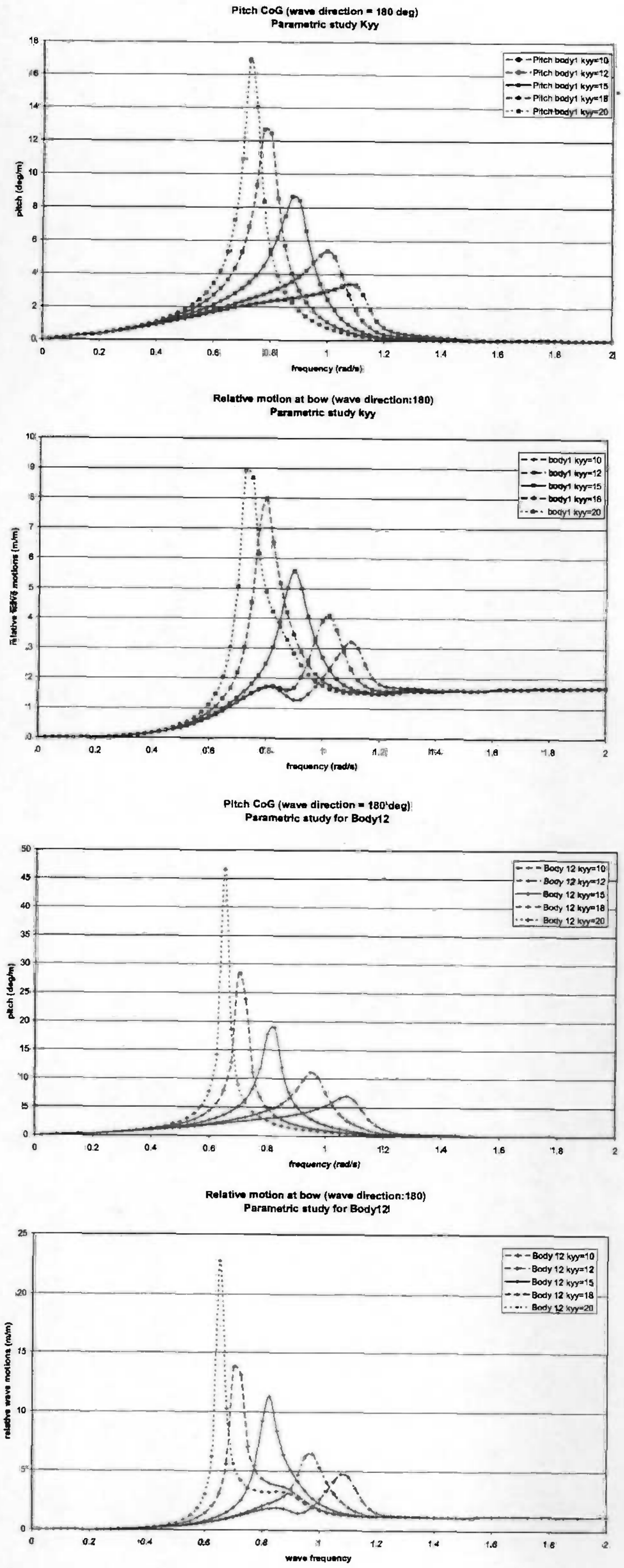

Figure 19 Effect of kyy variation on pitch motions and relative wave motions of body 1 (above) and body 12 (below)

So apart from the importance of a maximum pitch exciting moment and minimum wave damping, the natural period of the response is very important. As can be seen for body 1 (top graph of Figure 18) for this body the pitch peak response is not the same as the point of maximum pitch excitation. For body 12 this is better, but still not exact.

Therefore, a systematic variation of the pitch radius of gyration was carried out for bodies 1 and 12. Figure 19 shows the effect of this kyy variation on the pitch motions and relative wave motions of body 1 (above) and body 12 (below). A realistic range of kyy was chosen (based on possible water ballast and structural weight): 10m, 12m, 15m, 18m and 20m. This resulted in natural pitch periods of 5.64s-8.23s (1.11-0.76 rad/s) for body 1 and 5.73s-9.29s (1.1-0.68 rad/s) for body 12. The results in Figure 19 make clear that this allows the tuning of the peak response to the area of maximum wave excitation (and minimum wave damping) and to adjust the 'Inverse concept' to the period of the incoming waves. Variation of the pitch natural period with the GM value (height of the centre of gravity) is not a real option, as the transverse GM values are limited (see Table 2) and needed for transverse stability.

So far the motion behaviour has only been studied based on (RAO) graphs. To better understand the implications of these results, it is also useful to visualise the waves and motions. This is done in Figure 20 for body 1 and 12 using the motions and wave field of the linear diffraction analysis.

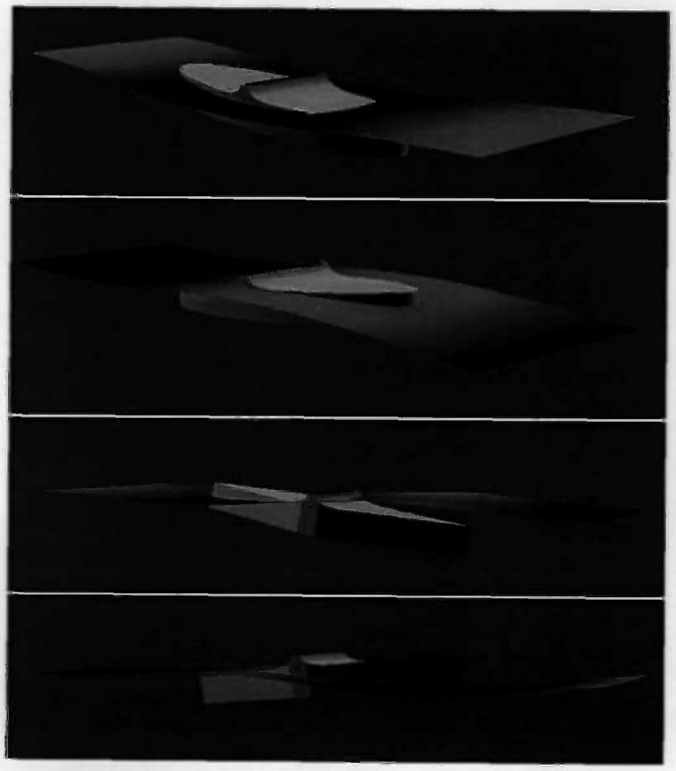

Figure 20 Visualisation of the behaviour of body 1 (top) and 12 (bottom) using the motions and disturbed wave field of the linear diffraction analysis (above calm level body part only present in visualisation)

The Figures confirm the large motions and relative wave motions presented in previous graphs. The bow makes large vertical motions and both the bow and stern submerge as as a result of the large relative wave motions.

It is important to note that in these Figures everything above the calm level is only added for visualisation purposes and neglected in the actual underlying diffraction analysis. Especially the water shown on top of the deck is unrealistic as a result. These Figures show that green water will flow onto the deck, but not how. For this purpose the next series of simulations with the improved Volume of Fluid (iVOF) method are necessary.

INITIAL IVOF SIMULATION OF GREEN WATER

The iVOF method in the ComFLOW program (developed by the University of Groningen, RuG) is based on the Navier-Stokes equations for an incompressible, viscous fluid. The equations are discretised using the finite volume method. The displacement of the free surface is done using the Volume of Fluid method first introduced by Hirt and Nichols [3-5]. To avoid small droplets disconnecting from the free surface, the iVOF-method is combined with a local height function. The iVOF method has already been used for a number of applications, like sloshing on board tumbling spacecraft, and blood flow through arteries. Maritime applications are sloshing in anti-roll tanks, green water flow on the deck, TLP response to extreme waves and falling objects in calm water [1, 3-5].

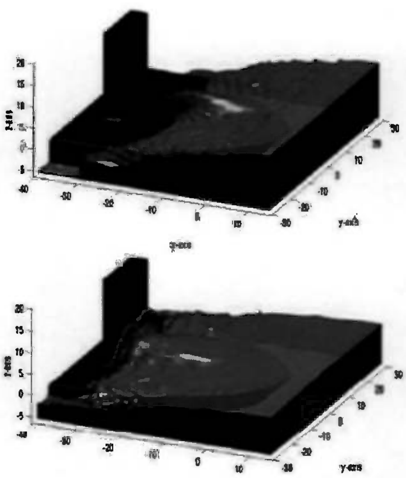

Figure 21: Visualisation of a green water simulation on an FPSO with the iVOF method [1], compare to the tests in Figure 3.

In [1,3] the results were shown of the simulation of the flow of green water over the deck of an FPSO and the resulting impact on deck structures. The computational domain was limited to the area on and around the deck. The freeboard exceedance around the deck was used as boundary condition and the deck was not moving in this approach. For the present initial simulations the same quasi-static approach has been used. In the next phase also the motions of the structure will be taken into account, as was done for an FPSO in [4] and TLP in [5]. However, the good results presented in Figures 21 and 22 (from [1]) for the flow onto the deck and the impact loading on the structure on the deck (see also Figure 3), justify the use of this approach at this stage of the 'Inverse' project.

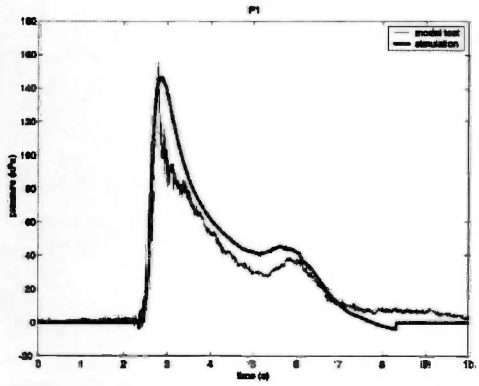

Figure 22: Comparison between the simulated and measured green water impact on the structure on the deck [1].

Figure 23 shows the description of bodies 1 and 12 as input for the iVOF simulation. The main body, the slopes, the reservoir and the outflow openings are modelled.

For the present initial simulations only half the body was used. As starting/boundary condition of the simulation a stationary 'wall' of water around the structure is chosen of 5.0m high above the deck level. Considering the freeboard level assumed (2.0m), this requires a relative wave motion of 7.0m. Based on the relative wave motion results presented in Figure 19, this will regularly occur in significant wave heights in the order of 2-3m.

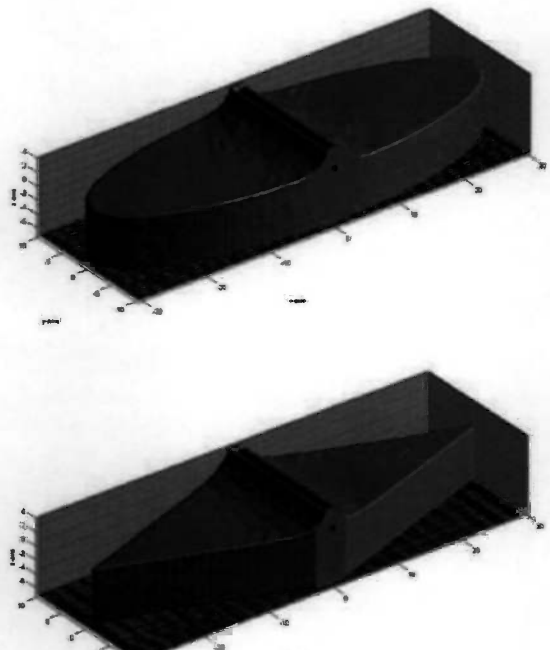

Figure 23: Modelling of body 1 and body 12 for the iVOF simulation.

The different stages of the flow onto the deck are shown in Figure 24 for the elliptical body 1 and in Figure 25 for the triangular body 12. The Figures start with the initial condition at the beginning of the simulation. Then both bodies shows the required behaviour where water from the fronts and sides of the bow flows towards to the centreline, where it forms a high velocity water jet over the deck. The water runs up the slope of the deck and then flows into the top of the reservoir. The reservoir collects the water and the water flows out of the openings at the side, at which lower head turbines will be placed. At present a simple squared reservoir was used. In reality an optimised vertical funnel shaped structure will be used to maximise the pressure head.

It will be clear from Figures 24 and 25 that the shape of the deck in plan view has a large effect on the flow on the deck itself. The triangular shape of body 12 with its sharp apex seems particularly effective to combine the two waterfronts of the sides into a jet along the centreline.

It should be noted that in reality the green water flows onto a moving deck. The pitching motion of the structure (bow up after the green water has flown onto the deck) will increase the flow velocity of the water over the deck into the reservoir. Further the green water flow will occur both from the bow and the stern. As the green water flow onto the deck is mainly a dam-breaking type of flow [1], the green water velocities are mainly a result of the local relative wave elevation and less influenced by the orbital motion of the waves. In that respect similar flow from the bow and stern is expected, except for the difference in relative wave motions (which are affected by wave reflection, although this will be small for the thin body 12).

CONCLUSIONS

The paper presented the initial investigations into the 'Inverse' concept for wave energy conversion, using on the maximisation of motions and green water. Based on the results presented, the following initial conclusions seem justified:

- The 'Inverse' concept combines aspects of 'overtopping', 'heaving' and 'pitching' concepts for wave energy conversion, but also adds specific aspects such as the use of green water.
- An increased draft of the structure increases the pitch motions and relative wave motions. This can be explained by the fact that the pitch excitation reduces less with the increasing draft than the wave damping. A reduced wave damping is attractive as this implies that less energy is dissipated by the wave radiation and can be used for actual wave energy conversion.
- By changing the inertia (radius of gyration) of the structure, the natural pitch period can be tuned to the frequency at which the highest wave exciting pitch moment occurs. This is important as it allows us to adjust the 'Inverse concept' to the period of the incoming waves. At resonance the spring terms in

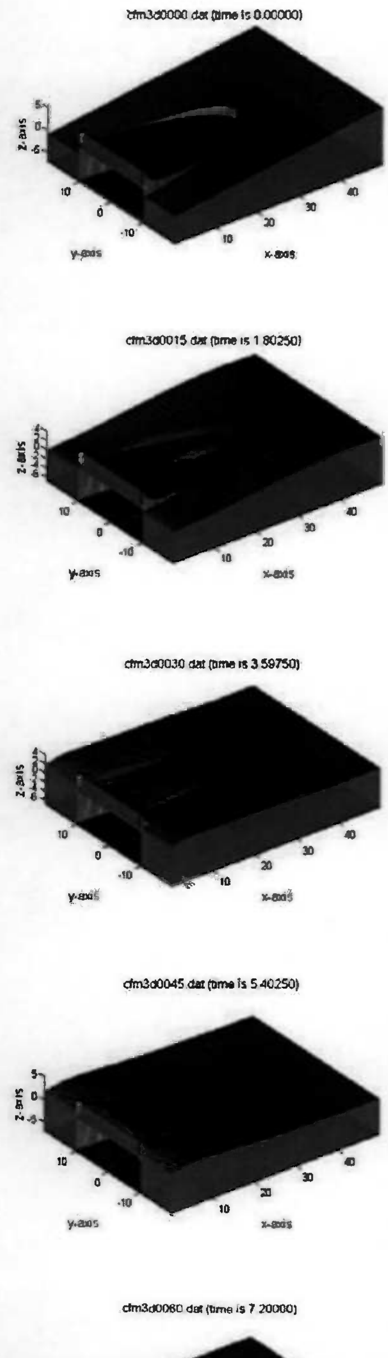

Figure 24: Flow onto the deck and into the reservoir for body 1 with a freeboard exceedance of 5.0m

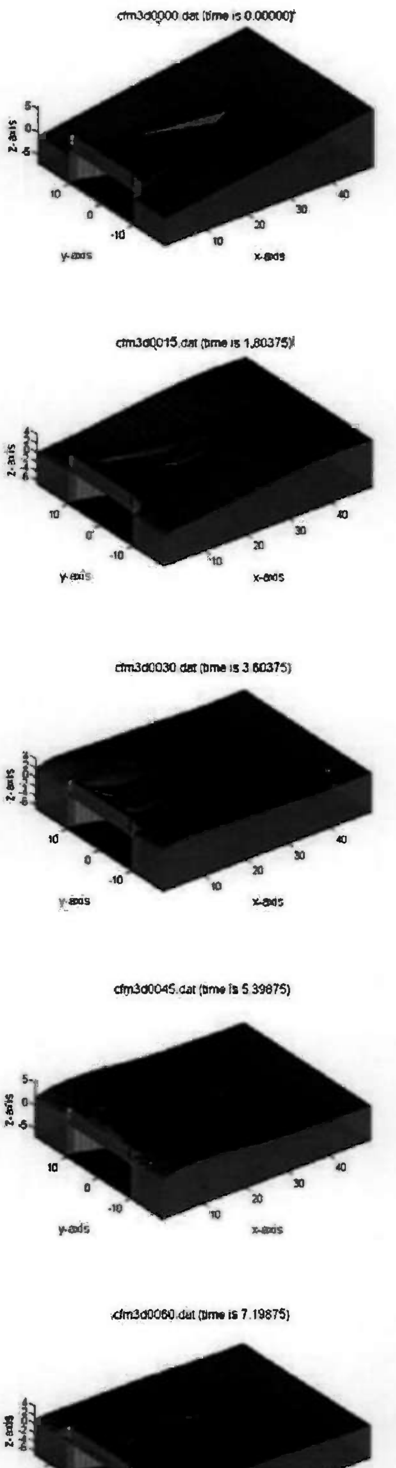

Figure 25: Flow onto the deck and into the reservoir for body 12 with a freeboard exceedance of 5.0m

the equation of motion are cancelling the inertia terms, which results in a maximum response. The actual motion response is based on the balance between the wave excitation and the damping. In the present simulations only the wave damping is considered. In the future also the damping as a result of the electrical generator has to be taken into account.

- The iVOF simulations finally have shown that the principle of concentrated green water flow over the centreline of a structure can be used to fill a reservoir.

Summarizing, it can be concluded that the principles of the 'Inverse' concept have been proved. As a result of the double connotation of the word 'green', this renewable energy concept could also be called the 'green water' concept.

Further work needs to be carried out on the optimisation of the concept. In the next phases also the actual energy generation capabilities of the 'Inverse' concept will have to be studied in detail, considering the characteristics of the electrical generator in the time domain and its effect on the motions of the structure. Further the flow of the greenwater into the reservoir on the moving structure has to be optimised. Finally the survivability of the structure in extreme conditions has to be investigated, also considering the loads in the mooring system.

REFERENCES

1. Buchner, B.: "*Green water on ship-type offshore structures*", PhD thesis, Delft University of Technology, 2002.
2. 'Ocean Energy Conversion in Europe, Recent advancements and prospects', Published in the framework of the "Co-ordinated Action on Ocean Energy" (http://www.ca-oe.org) EU project under FP6 Priority: Renewable Energy Technologies, Centre for Renewable Energy Sources, 2006
3. Fekken, G., Veldman, A.E.P. and Buchner, B.: "*Simulation of green-water loading using the Navier-Stokes equations*", Proceedings 7th Intern. Conf. on Numerical Ship Hydrodynamics, Nantes, 1999.
4. Kleefsman, K.M.T. and Veldman, A.E.P.: "*An improved {V}olume of {F}luid i{VOF} method for wave impact type problems*", Proceedings of OMAE-FPSO 2004.
5. Johannessen, T.B., Haver, S., Bunnik, T.H.J and Buchner, B.: *"Extreme Wave Effects on Deep Water TLPs Lessons Learned from the Snorre A Model Tests"*, DOT Conference, Houston, 2006.